JBC Papers in Press. Published on March 10, 2010 as Manuscript M109.098400
The latest version is at http://www.jbc.org/cgi/doi/10.1074/jbc.M109.098400

MITOCHONDRIAL AND NUCLEAR GENOMIC RESPONSES TO LOSS OF *LRPPRC* EXPRESSION

Vishal M. Gohil[1,2,3], Roland Nilsson[1,2,3], Casey A. Belcher-Timme[1,2,3], Biao Luo[2], David E. Root[2], Vamsi K. Mootha[1,2,3]

[1]Center for Human Genetic Research, Massachusetts General Hospital, Boston, MA 02114 USA
[2] Broad Institute of MIT and Harvard, Cambridge, MA 02142 USA
[3] Department of Systems Biology, Harvard Medical School, Boston, MA 02446 USA

Address correspondence to: Vamsi K. Mootha, MGH Center for Human Genetic Research, 185 Cambridge Street CPZN 5-806, Boston, MA 02114 USA. t: 617-643-3096; f: 617-643-2335; e: vamsi@hms.harvard.edu

Rapid advances in genotyping and sequencing technology have dramatically accelerated the discovery of genes underlying human disease. Elucidating the function of such genes and understanding their role in pathogenesis, however, remains challenging. Here, we introduce a genomic strategy to functionally characterize such genes, and apply it to *LRPPRC*, a poorly studied gene that is mutated in Leigh Syndrome, French-Canadian type (LSFC). We utilize RNAi to engineer an allelic series of cellular models in which *LRPPRC* has been stably silenced to different levels of knockdown efficiency. We then combine genome-wide expression profiling with gene set enrichment analysis (GSEA) to identify cellular responses that correlate with the loss of *LRPPRC*. Using this strategy, we discovered a specific role for *LRPPRC* in the expression of all mitochondrial DNA (mtDNA)-encoded mRNAs, but not the rRNAs, providing mechanistic insights into the enzymatic defects observed in the disease. Our analysis shows that nuclear genes encoding mitochondrial proteins are not collectively affected by the loss of *LRPPRC*. We do observe altered expression of genes involved in hexose metabolism, prostaglandin biosynthesis, and glycosphingolipid biology that may either play an adaptive role in cell survival or contribute to the disease pathogenesis. The combination of genetic perturbation, genomic profiling and pathway analysis represents a generic strategy for understanding disease pathogenesis.

Over the last few years, the discovery of genes associated with human disease has progressed rapidly with the advent of new genomic technologies including single nucleotide polymorphism (SNP) arrays and next generation sequencing. Genome-wide association studies (GWAS) aided by SNP arrays have yielded a plethora of genes associated with common diseases like cancer and diabetes (1). Integrative genomic approaches made possible by the availability of large-scale biological data sets have hastened the discovery of causative genes for rare Mendelian disorders (2). More recent advances in sequencing technologies further promise rapid identification of a multitude of mutant alleles responsible for Mendelian disorders as exemplified by the discovery of *DHOD* mutations in Miller syndrome (3). Still, pinpointing the exact function of newly discovered genes and the global implications of mutations on cellular function remains extremely challenging. The identification of causative alleles is an important first step in the diagnosis of a disorder; however, determining gene function and characterizing cellular responses to disease-causing mutations is necessary to fully understand disease pathogenesis. In the post-genomic world, the latter step remains a major bottleneck.

One of the first successful applications of GWAS was Leigh syndrome, French-Canadian type (LSFC) (4). LSFC is a rare, monogenic, Mendelian mitochondrial disease that presents as a cytochrome c oxidase (COX) deficiency, common in the Saguenay-Lac-Saint-Jean region of Quebec.

Lee *et al.* mapped the disease to a 2 cM region on chromosome 2 by performing a genome-wide screen for linkage disequilibrium (4). A follow-up integrative genomic analysis spotlighted *LRPPRC,* leucine-rich pentatricopeptide repeat-motif containing protein, a high-scoring candidate gene whose product is co-expressed with known mitochondrial genes (5). Subsequent sequencing of *LRPPRC* identified two different causal mutations (5). *LRPPRC* encodes a 130 kDa RNA-binding protein (6) that localizes primarily to the mitochondria (5,6). It belongs to a family of pentatricopeptide repeat (PPR) proteins common to mitochondria and chloroplast that are particularly abundant in plants (7). As a class, PPR proteins tend to be sequence-specific RNA-binding proteins with direct roles in RNA editing, processing, splicing, and translation (8).

The precise molecular function of LRPPRC has remained controversial. Consistent with the predicted function of a PPR domain-containing protein, Xu *et al.* have shown that LRPPRC is required for the expression of mitochondrial DNA (mtDNA)-encoded COX subunits *CO1* and *CO3* (9). However, Cooper *et al*. proposed a role for LRPPRC in transcriptional activation of nuclear genes via its interaction with PGC-1α (10,11). The global effect of loss of *LRPPRC* on cellular metabolic pathways has not been determined, though previous reports have implicated *LRPPRC* in hepatic glucose homeostasis and brown fat differentiation (10,11). Like most rare diseases, unraveling the LSFC disease pathogenesis and determining the function of *LRPPRC* is hindered by the limited availability of patient samples. Since LSFC is characterized by a loss of function of *LRPPRC*, gene silencing by RNAi offers a tractable approach to create cellular models of LSFC disease.

Here, we use shRNA-mediated graded knockdown of *LRPPRC* to construct cellular models of LSFC that recapitulate all the reported disease phenotypes. To systematically identify mitochondrial and nuclear responses to loss of *LRPPRC*, we carry out genome-wide expression profiling of these cellular models, followed by gene set enrichment analysis (GSEA) (12). We demonstrate that all mtDNA-encoded mRNA transcripts decrease in proportion to the loss of *LRPPRC*. In contrast, mtDNA-encoded rRNAs are unaffected, suggesting a specific role for LRPPRC in mt-mRNA homeostasis. In addition, we find up-regulation of key enzymes for fructose and mannose metabolism and of genes for prostaglandin biosynthesis, as well as down-regulation of genes for glycosphingolipid biosynthesis. These pathways could play a compensatory role in the face of mitochondrial dysfunction, or alternatively may contribute to pathogenesis.

EXPERIMENTAL PROCEDURES

Cell culture

MCH58 immortalized human skin fibroblasts were cultured in high glucose DMEM (Invitrogen Cat. No. 11995) supplemented with 10% fetal bovine serum (Sigma Cat. No. F6178) and 1X penicillin, streptomycin, and glutamine (Invitrogen Cat. No. 10378-016). The cell culture media was further supplemented with 2 μg/ml puromycin and 50 μg/ml uridine to culture cells post lenti-viral infection.

Materials

Quantitative real-time PCR (qRT-PCR) assays for mitochondrial transcripts were developed in collaboration with Applied Biosystems (Foster City, CA). Antibodies including CO2, NDUFB8, SDHB, UQCRC2, ATP5A and VDAC1 were purchased from Mitosciences (Eugene, OR), β-Actin was obtained from Sigma (St. Louis, MO) and LRPPRC antibody was a generous gift from Serafin Pinol-Roma. cDNA synthesis SuperScript III kit was from Invitrogen (Cat. No. 11752). Human U133 plus 2.0 oligonucleotide array was purchased from Affymetrix (Santa Clara, CA).

shRNA lentivirus production and infection

Lentiviral vectors for expressing shRNA (pLKO.1) were constructed at the Broad Institute's RNAi platform (13). The shRNA sequences are shown in Supplementary Table 1. For infection, 200,000 cells were seeded in a 6-well dish. 30 μl viral supernatant was added to cells for a final volume of 2 ml media containing 8 μg/ml polybrene. The plates were spun at an RCF of 805 x g for 30 minutes at 32°C, returned to 37°C, and 24 hours post-infection were selected for infection using 2 μg/ml puromycin.

Quantitative real-time PCR

RNA was isolated from cells using the RNeasy kit (Qiagen). 500 ng of RNA was used as starting material to synthesize first-strand cDNA. 1 ng of genomic (g) DNA, isolated using the DNeasy kit (Qiagen), was used as starting material for the multiplex qRT-PCR assay to quantify mitochondrial DNA as previously described (14). qRT-PCR was performed on cDNA and gDNA samples using a 96-well ABI7500 real-time PCR system in 20 µl reactions prepared with 2X master mix, 20X ABI Taqman assay (Supplementary Table 2) and diluted cDNA or gDNA samples.

Western blotting

15-25 µg of protein sample was loaded per lane on a 4-12% Bis-Tris gel followed by electrophoresis at constant voltage (200V) for 50 min. The separated proteins were blotted onto a PVDF membrane and blocked for one hour at room temperature in tris-buffered saline with 0.1% Tween-20 and 5% BSA (TBST-BSA). Membranes were incubated with primary antibody in TBST-BSA overnight at 4°C. Primary antibodies were used at the following dilutions: LRPPRC (1:500), β-Actin (1:10,000), CO2 (1:2,000), NDUFB8 (1:500), SDHB (1:500), UQCRC2 (1:1,000), ATP5A (1:10,000), and VDAC1 (1:1,000). Secondary antibody was used at (1:5,000) for one hour at room temperature. Membranes were developed using WesternLightning Plus-ECL.

Measurement of cellular oxygen consumption and extracellular acidification

Oxygen consumption rate (OCR) and extracellular acidification rate (ECAR) measurements were carried out as previously described (15) with minor modifications. *LRPPRC* knockdown cells were seeded in XF 24-well cell culture microplates (Seahorse Bioscience) at 30,000 cells/well and incubated at 37°C and 5% CO_2 for 24 h. Prior to measurement, the growth medium was replaced with 925 µl of assay medium (Seahorse Bioscience). The cells were incubated at 37°C for 60 min in the assay medium prior to measurements. The OCR and ECAR measurements were taken simultaneously every 7 minutes after a 2 minute mix and a 2 minute wait period.

Microarray analysis

Total RNA was extracted from ~ 2 million cells with RNeasy mini kit (Qiagen). 10 µg of RNA was used to synthesize cDNA with a T7-$(dT)_{24}$ primer and the SuperScript one-cycle cDNA synthesis kit (Affymetrix). cRNA labeling, hybridization to human U133 plus 2.0 oligonucleotide array, washing, and staining were performed as recommended by Affymetrix. Two biological replicates were used for each *LRPPRC* knockdown cell line, for a total of 14 arrays. Microarray data were analyzed using GSEA to identify pathways whose expression was altered in concert with the expression of *LRPPRC*. We used metabolic pathways defined by Edinburgh Human Metabolic Network (16) as well as a set of U133 plus 2.0 probes targeting mtRNA transcripts, nuclear-encoded oxidative phosphorylation (OXPHOS) genes as described previously (14) and a gene set comprised of all the nuclear-encoded mitochondrial proteins as defined in MitoCarta (17).

RESULTS

Engineering and Validating Cellular Models of LSFC

We designed seven shRNAs targeting *LRPPRC* cDNA sequence to silence its expression in MCH58 immortalized human skin fibroblasts. We chose diploid human fibroblasts to construct stable cellular models since it has been previously shown for a number of mitochondrial diseases including LSFC that fibroblasts do express biochemical phenotypes associated with disease mutations (Supplementary Table 3). We quantified *LRPPRC* transcript level by qRT-PCR measurement on RNA extracted from shLRPPRC infected cells. As shown in Fig. 1A, the extent of knockdown was hairpin-specific and the *LRPPRC* transcript level ranged from 8% to 100% in knockdown cell lines. Moreover, depletion of LRPPRC protein was strongly correlated with the pattern of progressive mRNA knockdown (Fig. 1B). One classical biochemical feature of LSFC is a reduced level of COX subunits (18). To demonstrate that our knockdown cell lines faithfully model LSFC, we carried out Western blot analysis for CO2, an mtDNA-encoded subunit of COX, and confirmed that depletion of LRPPRC

results in a corresponding and proportional reduction of CO2 (Fig. 1C). To further demonstrate that our knockdown cells recapitulate the physiological defects associated with LSFC, we interrogated oxidative and glycolytic metabolism by assaying for oxygen consumption rate (OCR) and extracellular acidification rate (ECAR), respectively. As expected, decreasing *LRPPRC* mRNA levels produced a quantitatively correlated decrease in the ratio of OCR to ECAR, indicating a coordinated decrease in respiration and an increase in glycolytic output (Fig. 1D). The knockdown of LRPPRC and the resulting depletion of CO2 in lentiviral-shRNA infected cell lines persisted over the course of ten passages, approximately one month after infection, demonstrating that our cell lines are indeed stable (Fig. 1E).

Mitochondrial and Nuclear Transcriptional Response in Cellular Models of LSFC

We performed genome wide expression profiling of the engineered LSFC cell lines to systematically identify biochemical pathways that are altered in response to the depletion of *LRPPRC* and the consequent loss of mitochondrial respiratory function. The *LRPPRC* transcript levels determined by microarray analysis were strongly correlated with those obtained by qRT-PCR (Pearson's correlation coefficient = 0.99) (Supplementary Fig. 1), suggesting that the expression profiling data is of high quality. We performed GSEA on the expression data from the seven engineered LSFC cell lines, each with progressively decreased *LRPPRC* expression. GSEA identified seven gene sets that are significantly correlated with *LRPPRC* expression at a nominal *P*-value less than 0.05 and a false discovery rate of less than 25% (Fig. 2). The mtRNAs gene set was strongly positively correlated with *LRPPRC* expression and exhibited a nearly perfect enrichment score (1.00) (Fig. 2A,C). Among the nuclear-encoded gene sets, three were positively correlated with *LRPPRC* expression: "O-glycan biosynthesis", "glycosphingolipid biosynthesis" and "glycosphingolipid metabolism" (Fig. 2A). The negatively correlated gene sets were "fructose and mannose metabolism", "putative anti-inflammatory metabolite formation from eicosapentanoic acid (EPA)" and "prostaglandin formation from arachidonate" (Fig 2B). Notably, the nuclear-encoded OXPHOS gene set (ES = -0.25; P = 0.79) (Fig. 2C) and the gene set comprised of all nuclear-encoded mitochondrial proteins (ES = 0.16; P = 0.90) did not show significant correlation.

The highest-scoring negatively correlated gene set, annotated as "fructose and mannose metabolism", consist of genes involved in the synthesis of mannose-6-phosphate, GDP-mannose and GDP-fucose that are all intermediates in the glycoprotein biosynthesis. The same gene set also includes numerous genes encoding glycolytic enzymes (Supplementary Fig. 2A). The increased expression of glycolytic genes is likely a biochemical adaption to compensate for the loss of mitochondrial energy generating capacity. In support of this hypothesis, we found that *LRPPRC* knockdown cells were more sensitive to the glycolytic inhibitor 2-deoxyglucose compared to the control cell line (Supplementary Fig. 2B). The second- and third-ranking negatively correlated gene sets shared several genes encoding enzymes involved in prostaglandin biosynthesis, including the key enzyme cyclooxygenase 2 (PTGS2) (Supplementary Fig. 3).

Role of *LRPPRC* in the Regulation of mtDNA Encoded Transcripts

Although it has previously been shown that LRPPRC is necessary for the maintenance of steady-state levels of the mtDNA-encoded subunits of COX (9), we observed reduced expression of almost all of the mtDNA-encoded transcripts, including subunits of respiratory complex I (ND2-ND5), IV (CO1-CO3) and V (ATP6) (Fig. 3A). The reduced expression of these genes was not caused by mtDNA depletion, since the two most potent knockdowns, kd1 and kd6, had the same mtDNA content as control cells (Fig. 3B). In order to determine the precise role of LRPPRC in mitochondrial gene expression we designed multiple qRT-PCR Taqman assays that specifically probe each of the mtDNA-encoded mRNAs and rRNAs, as well as the polycistronic RNA transcript (Fig. 3C). The qRT-PCR measurement for mRNAs from the two most potent knockdown cell lines showed a significant depletion of each of the 13 mRNAs encoded by

the mtDNA (Fig. 3D). However, the expression of the two mtDNA-encoded rRNAs was unaffected by the loss of *LRPPRC* (Fig. 3D). The mitochondrial mRNAs are generated simultaneously as a polycistronic transcript from the heavy strand (HS) and light strand (LS) promoters (19). However, the mitochondrial rRNAs can be transcribed either as a part of this polycistronic transcript, or independently from the HSP1 promoter (19). The differential regulation of mRNAs and rRNAs in LSFC cell lines could either be due to promoter-specific transcriptional activation by LRPPRC, or LRPPRC may act post-trancriptionally on mRNAs. To differentiate between these scenarios, we designed a qRT-PCR assay that specifically probes the polycistronic transcripts (Fig. 3C). We observed no reduction in polycistronic transcript level in the *LRPPRC* knockdown cells (Fig. 3D), suggesting that LRPPRC acts downstream of the polycistronic transcript to maintain steady-state mRNA levels. Finally, we verified that the reduction in mitochondrial mRNA results in defective respiratory complex assembly, using a Western blot assay for a labile subunit of each respiratory complex (14). We observed depletion of complex I, III, and IV subunits in the two cell lines with most potent *LRPPRC* knockdown (Supplementary Fig. 4).

DISCUSSION

It has been more than six years since *LRPPRC* has been identified as a causative gene for LSFC, yet its precise function has remained unclear. Based on the presence of a PPR motif, sequence similarity to the yeast PET309 protein, and the mitochondrial localization of LRPPRC, Mootha *et al*. postulated a mRNA-processing role for LRPPRC (5). Indeed, a subsequent study on LSFC patient fibroblasts showed a selective decrease in mtDNA-encoded *CO1* and *CO3* transcripts (9). This finding is consistent with the COX enzyme deficiency in LSFC patients. However, our study shows that LRPPRC is required for the expression of all the mtDNA-encoded mRNA and is not specific to COX subunits. This discordance may be due to differences in LRPPRC protein levels; that is, a more severe depletion in our knockdown cellular models compared to a milder decrease in LSFC patients with a point mutation in *LRPPRC*. These results imply that stimulating LRPPRC expression in LSFC patients may prove beneficial. Importantly, we have shown that LRPPRC depletion does not alter transcript levels of rRNA (Fig. 3D), suggesting a specific role for LRPPRC in the processing of mitochondrial mRNAs. At present, the exact molecular function of LRPPRC is not known. It is likely that other proteins may interact with LRPPRC to co-stabilize mRNA. In this regard it is noteworthy that the loss of SLIRP, a RNA-binding protein, results in a remarkably similar pattern of mitochondrial mRNA depletion (14).

Mitochondrial disorders are frequently characterized by a variety of clinical features that are not readily linked to the biochemical defect within the respiratory chain. Our engineered LSFC cell lines offer a powerful tool to discover cellular responses that may help understand this pathogenesis. This approach is effective because LRPPRC protein appears to be limiting in cells: a decrease in its level strongly correlates with mitochondrial mRNA expression (Fig. 3A) and cellular energetics (Fig. 1D). The allelic series of *LRPPRC* knockdown cell lines offers multiple advantages: it cancels the off-target effects of individual shRNAs; it provides an isogenic background that eliminates genotype specific effects; stable silencing allow us to understand the long-term adaptations of the cell to the loss of gene function; and it recapitulates the phenotypes observed in mitochondrial disease where mitochondrial respiration is defective. The transcriptional responses to a graded loss of LRPPRC and reduced mitochondrial function may be either dose-dependent or exhibit a threshold behavior. By analyzing gene expression data based on linear (Pearson) correlation with the *LRPPRC* expression level, the current analysis is focused on dose-dependent responses; however, our data could be re-analyzed with different similarity metrics to identify genes exhibiting non-linear responses as well. Of the pathways showing a dose-dependent response, we were particularly interested in gene sets that were negatively correlated with *LRPPRC* expression, since these may represent activation of an adaptive cellular response to the loss of mitochondrial energy generating capacity. We found three such anti-correlated, statistically significant gene sets (Fig.

2B), representing hexose sugar metabolism and prostaglandin biosynthesis. The hexose sugar metabolism gene set included key glycolytic genes such as *HK1*, *HK2* and *HK3*. Previous studies have shown increased expression of genes involved in glycolysis, including *HK1*, *HK2*, *LDHB*, and *PFK* in mtDNA mutant cells (20,21). The up-regulation of these genes likely facilitates increased ATP production via glycolysis, a necessary adaptation to the loss of mitochondrial respiratory capacity observed in mitochondrial disorders including LSFC. Indeed, LSFC cells displayed greater sensitivity to a glycolytic inhibitor (Supplementary Fig. 2B). Notably, the gene set comprised of hexose sugar metabolism includes genes required for the synthesis of GDP-mannose and GDP-fucose which provide a carbohydrate backbone for glycoprotein synthesis. The increased expression of genes encoding this pathway suggests alterations in glycoprotein biosynthesis upon mitochondrial dysfunction.

The concerted up-regulation of genes involved in the prostaglandin (PG) biosynthetic pathway was surprising. Upon literature survey, we found recent reports that link PG biosynthesis to mitochondrial dysfunction. First, Cillero-Pastor *et al*. showed that treatment of primary human chondrocytes with the respiratory inhibitors oligomycin or antimycin stimulated PTGS2 expression and PGE_2 production (22). Second, Tomura *et al.* have shown that acidification of culture media results in an increase in PTGS2 expression and a corresponding increase in PGE_2 synthesis (23). The up-regulation of the prostaglandin pathway is also consistent with the retrograde signaling hypothesis, which states that mitochondrial dysfunction results in increased cytosolic Ca^{2+}, which stimulates calcineurin leading to the activation of NF-κB (24), a key transcriptional activator of PG biosynthetic genes. The up-regulation of PG biosynthetic genes could be adaptive, since PGE_2 inhibits apoptosis, up-regulates a number of pro-survival pathways including PI3K/AKT and ERK, and stimulates VEGF expression through activation of HIF1α (25). Thus, PGE_2 biosynthesis could play a cytoprotective role in respiratory compromised cells.

In previous studies, Cooper *et al.* have shown that LRPPRC interacts with PGC-1α to stimulate the expression of a subset of nuclear-encoded mitochondrial genes in mouse primary hepatocytes and brown fat cells (10,11). All shLRPPRC hairpins used in this study are predicted to silence mitochondria-targeted LRPPRC as well as LRPPRC targeted to the nucleus/cytosol. However, our GSEA analysis of LSFC cell lines did not detect any effect on expression of the nuclear-encoded mitochondrial genes that are targets of PGC-1α including the OXPHOS genes (Fig. 2C). This discrepancy could be due to differences between cell types. Although our data strongly favors a role for LRPPRC in regulating mitochondrial mRNAs, an additional nucleus-specific function cannot be ruled out.

In summary, we here report the construction of stable cellular models of LSFC disease in an isogenic background, and the discovery of a specific function of LRPPRC in mt-mRNA homeostasis. In addition, we identify nuclear-encoded pathways that could shed light on mitochondrial disease pathogenesis. Our approach overcomes a number of limitations of previous genomic profiling studies conducted on mitochondrial disease cells, where results were confounded by genetic heterogeneity and tissue diversity of samples (26). Our well-characterized LSFC disease models could serve as a valuable resource to understand mitochondrial disease pathogenesis through further investigation using proteomic analysis, metabolomic profiling and chemical screening.

REFERENCES

1. McCarthy, M. I., Abecasis, G. R., Cardon, L. R., Goldstein, D. B., Little, J., Ioannidis, J. P., and Hirschhorn, J. N. (2008) *Nat. Rev. Genet.* **9**, 356-369
2. Giallourakis, C., Henson, C., Reich, M., Xie, X., and Mootha, V. K. (2005) *Annu. Rev. Genomics Hum. Genet.* **6**, 381-406

3. Ng, S. B., Buckingham, K. J., Lee, C., Bigham, A. W., Tabor, H. K., Dent, K. M., Huff, C. D., Shannon, P. T., Jabs, E. W., Nickerson, D. A., Shendure, J., and Bamshad, M. J. (2010) *Nat. Genet.* **42,** 30-35
4. Lee, N., Daly, M. J., Delmonte, T., Lander, E. S., Xu, F., Hudson, T. J., Mitchell, G. A., Morin, C. C., Robinson, B. H., and Rioux, J. D. (2001) *Am. J. Hum. Genet.* **68**, 397-409
5. Mootha, V. K., Lepage, P., Miller, K., Bunkenborg, J., Reich, M., Hjerrild, M., Delmonte, T., Villeneuve, A., Sladek, R., Xu, F., Mitchell, G. A., Morin, C., Mann, M., Hudson, T. J., Robinson, B., Rioux, J. D., and Lander, E. S. (2003) *Proc. Natl. Acad. Sci. U. S. A.* **100**, 605-610
6. Mili, S., and Pinol-Roma, S. (2003) *Mol. Cell Biol.* **23**, 4972-4982
7. Lurin, C., Andres, C., Aubourg, S., Bellaoui, M., Bitton, F., Bruyere, C., Caboche, M., Debast, C., Gualberto, J., Hoffmann, B., Lecharny, A., Le Ret, M., Martin-Magniette, M. L., Mireau, H., Peeters, N., Renou, J. P., Szurek, B., Taconnat, L., and Small, I. (2004) *Plant Cell* **16**, 2089-2103
8. Schmitz-Linneweber, C., and Small, I. (2008) *Trends Plant Sci.* **13**, 663-670
9. Xu, F., Morin, C., Mitchell, G., Ackerley, C., and Robinson, B. H. (2004) *Biochem. J.* **382**, 331-336
10. Cooper, M. P., Qu, L., Rohas, L. M., Lin, J., Yang, W., Erdjument-Bromage, H., Tempst, P., and Spiegelman, B. M. (2006) *Genes Dev.* **20**, 2996-3009
11. Cooper, M. P., Uldry, M., Kajimura, S., Arany, Z., and Spiegelman, B. M. (2008) *J. Biol. Chem.* **283**, 31960-31967
12. Mootha, V. K., Lindgren, C. M., Eriksson, K. F., Subramanian, A., Sihag, S., Lehar, J., Puigserver, P., Carlsson, E., Ridderstrale, M., Laurila, E., Houstis, N., Daly, M. J., Patterson, N., Mesirov, J. P., Golub, T. R., Tamayo, P., Spiegelman, B., Lander, E. S., Hirschhorn, J. N., Altshuler, D., and Groop, L. C. (2003) *Nat. Genet.* **34**, 267-273
13. Moffat, J., Grueneberg, D. A., Yang, X., Kim, S. Y., Kloepfer, A. M., Hinkle, G., Piqani, B., Eisenhaure, T. M., Luo, B., Grenier, J. K., Carpenter, A. E., Foo, S. Y., Stewart, S. A., Stockwell, B. R., Hacohen, N., Hahn, W. C., Lander, E. S., Sabatini, D. M., and Root, D. E. (2006) *Cell* **124**, 1283-1298
14. Baughman, J. M., Nilsson, R., Gohil, V. M., Arlow, D. H., Gauhar, Z., and Mootha, V. K. (2009) *PLoS Genet.* **5**, e1000590
15. Wu, M., Neilson, A., Swift, A. L., Moran, R., Tamagnine, J., Parslow, D., Armistead, S., Lemire, K., Orrell, J., Teich, J., Chomicz, S., and Ferrick, D. A. (2007) *Am. J. Physiol. Cell Physiol.* **292**, C125-136
16. Ma, H., Sorokin, A., Mazein, A., Selkov, A., Selkov, E., Demin, O., and Goryanin, I. (2007) *Mol. Syst. Biol.* **3**, 135
17. Pagliarini, D. J., Calvo, S. E., Chang, B., Sheth, S. A., Vafai, S. B., Ong, S. E., Walford, G. A., Sugiana, C., Boneh, A., Chen, W. K., Hill, D. E., Vidal, M., Evans, J. G., Thorburn, D. R., Carr, S. A., and Mootha, V. K. (2008) *Cell* **134**, 112-123
18. Merante, F., Petrova-Benedict, R., MacKay, N., Mitchell, G., Lambert, M., Morin, C., De Braekeleer, M., Laframboise, R., Gagne, R., and Robinson, B. H. (1993) *Am. J. Hum. Genet.* **53**, 481-487
19. Bonawitz, N. D., Clayton, D. A., and Shadel, G. S. (2006) *Mol. Cell* **24**, 813-825
20. Heddi, A., Stepien, G., Benke, P. J., and Wallace, D. C. (1999) *J. Biol. Chem.* **274**, 22968-22976
21. Behan, A., Doyle, S., and Farrell, M. (2005) *Mitochondrion* **5**, 173-193
22. Cillero-Pastor, B., Carames, B., Lires-Dean, M., Vaamonde-Garcia, C., Blanco, F. J., and Lopez-Armada, M. J. (2008) *Arthritis Rheum.* **58**, 2409-2419
23. Tomura, H., Wang, J. Q., Liu, J. P., Komachi, M., Damirin, A., Mogi, C., Tobo, M., Nochi, H., Tamoto, K., Im, D. S., Sato, K., and Okajima, F. (2008) *J. Bone Miner. Res.* **23**, 1129-1139
24. Butow, R. A., and Avadhani, N. G. (2004) *Mol. Cell* **14**, 1-15
25. Greenhough, A., Smartt, H. J., Moore, A. E., Roberts, H. R., Williams, A. C., Paraskeva, C., and Kaidi, A. (2009) *Carcinogenesis* **30**, 377-386

26. Reinecke, F., Smeitink, J. A., and van der Westhuizen, F. H. (2009) *Biochim. Biophys. Acta* **1792,** 1113-1121

FOOTNOTES

This work was funded by grants from the United Mitochondrial Disease Foundation (VMG), the Broad Institute Scientific Planning and Allocation of Resources Committee, the American Diabetes Association, and the National Institutes of Health (R01DK081457) (VKM).

Abbreviations: LRPPRC, leucine rich pentatricopeptide repeat-motif containing protein; LSFC, Leigh Syndrome French Canadian variant

Acknowledgements: We thank Eric Shoubridge for the generous gift of MCH58 cell line, Olga Goldberger for technical assistance, Oded Shaham for assistance in designing qRT-PCR assays, Joshua Baughman and Scott Vafai for valuable discussion and comments, Serena Silver and Jennifer Grenier for assistance with shRNA work.

FIGURE LEGENDS

Figure 1. Using RNAi to engineer cellular models of LSFC. (A) *LRPPRC* mRNA quantified by qRT-PCR on MCH58 human fibroblasts infected with an empty vector, pLKO.1 (ctrl) or one of seven independent shRNAs targeting *LRPPRC*. Values are reported as fold change in expression over control (ctrl). Three biological replicates were used per hairpin (error bars represent standard deviation). β-Actin expression was used as an endogenous control. (B) Western blot detection of LRPPRC protein abundance in *LRPPRC* knockdown cell lines. (C) Western blot detection of CO2 protein abundance in *LRPPRC* knockdown cell lines. (D) Correlation between the ratio of oxygen consumption rate (OCR) to extracellular acidification rate (ECAR) and *LRPPRC* expression as measured in (A) ($n \geq 4$). (E) Western blot of LRPPRC and CO2 protein abundance over the course of five passages spanning approximately 15-30 days of culture after infection with pLKO.1 or one of the two most potent hairpin.

Figure 2. Gene set enrichment analysis of genomic profiles following *LRPPRC* knockdown. (A) List of gene sets that are positively correlated to *LRPPRC* expression. (B) List of gene sets that are negatively correlated to *LRPPRC* expression. Only gene sets that show ($p<0.050$ and FDR<0.250) are listed. (C) (Left) heat map showing expression of all 20,655 genes. Genes were ordered by their correlation to the *LRPPRC* expression profile (shown in black bars), with genes showing the strongest correlation at the top and the genes showing the strongest anti-correlation at the bottom. Red color indicates the highest expression and blue color indicates the lowest. (Right) bar plot indicating genes belonging to mitochondrial RNAs and nuclear OXPHOS genes.

Figure 3. LRPPRC is required for the maintenance of mitochondrial mRNAs. (A) Heatmap showing abundance of mitochondrial transcripts in LSFC cell lines as identified by micorarray. Two replicates of each knockdown are shown adjacent to each other. (B) mtDNA copy number as quantified by qRT-PCR for two most potent knockdowns and the pLKO.1 transduced control (ctrl) cell line. Values are reported as fold change over cells infected with pLKO.1. (n=3; error bars represent standard deviation from mean) (C) Schematic representation of qRT-PCR Taqman assay locations for mitochondrial transcripts. rRNA are indicated by blue, mRNA by grey, tRNA by red, and assay location by green. * denotes location of assay for polycistronic transcript. (D) Mitochondrial mRNA, rRNA and polycistronic RNA transcript were quantified for each of the two most potent knockdowns by qRT-PCR. Values are reported as fold change over control cells; β-Actin was used as endogenous control. (n=3; error bars represent standard deviation).

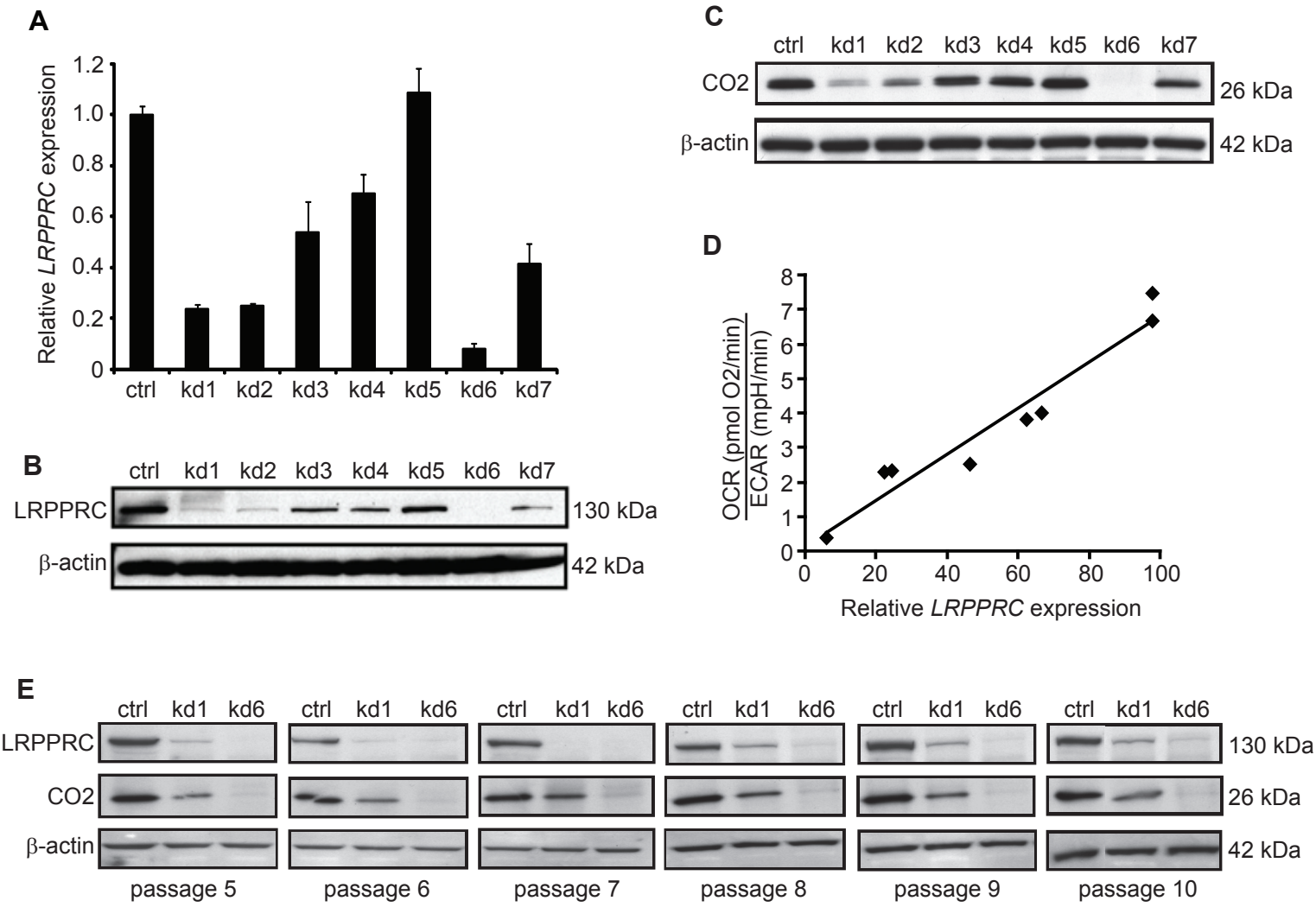

Figure 1

A

Positively Correlated Gene Sets (Size)	ES	*P*-Value
Mitochondrial RNAs (7)	1.00	0.00
O-Glycan biosynthesis (25)	0.57	0.02
Glycosphingolipid biosynthesis (25)	0.46	0.01
Glycosphingolipid metabolism (48)	0.40	0.02

B

Negatively Correlated Gene Sets (Size)	ES	*P*-Value
Fructose and mannose metabolism (24)	-0.63	0.00
Putative anti-inflammatory metabolite formation from EPA (19)	-0.58	0.01
Prostaglandin formation from arachidonate (47)	-0.47	0.04

C

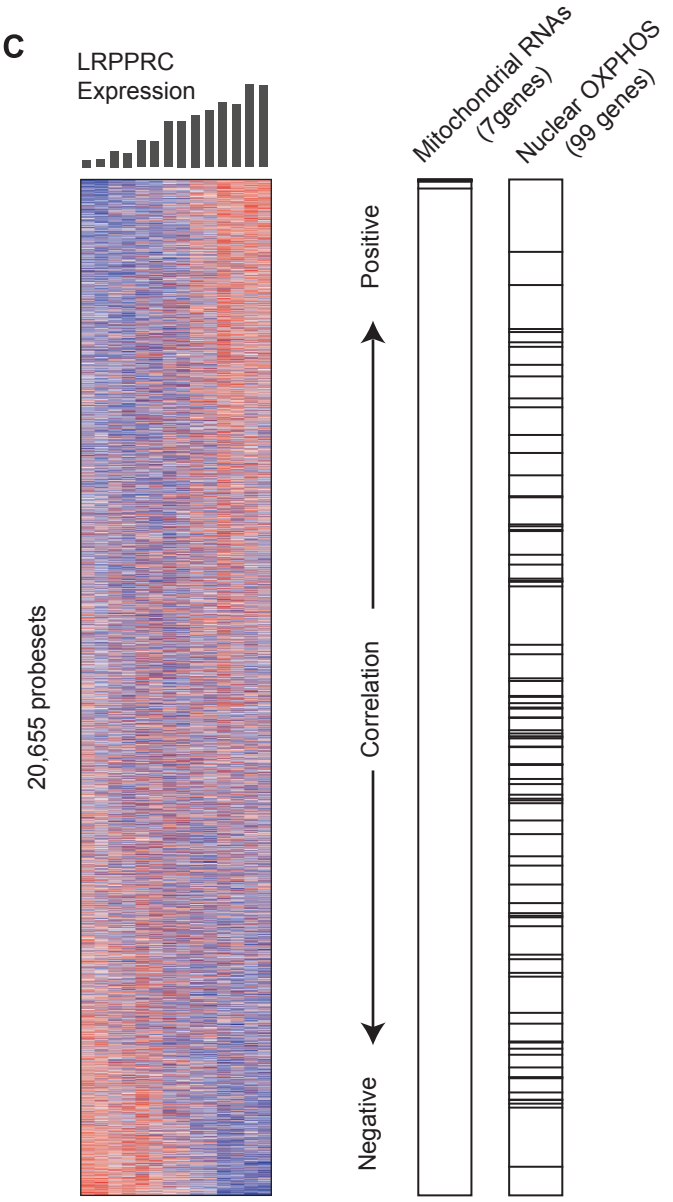

Figure 2

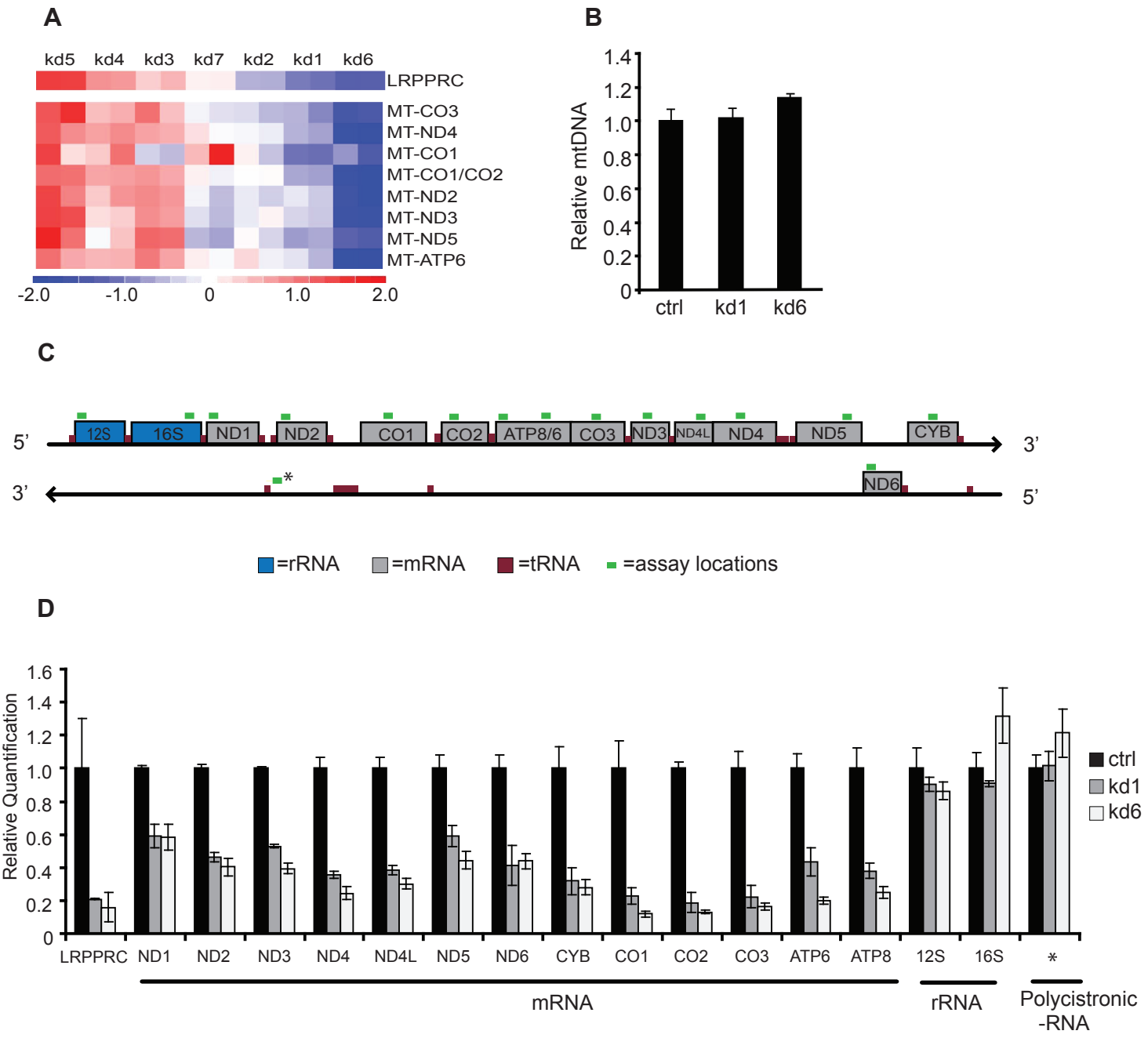

Figure 3